

***MULTIFUNCTIONAL ON-BOARD POWER
PROCESSOR WITH MULTIMODE CAPABILITIES
FOR ELECTRIC VEHICLE APPLICATIONS***



**Thesis submitted in partial fulfilment for the
Award of Degree**

Doctor of Philosophy

by

Virendra Prasad Maurya

**DEPARTMENT OF ELECTRICAL ENGINEERING
INDIAN INSTITUTE OF TECHNOLOGY
(BANARAS HINDU UNIVERSITY)
VARANASI - 221005**

ROLL NO.: 19081010

2025

CERTIFICATE

It is certified that the work contained in the thesis titled "*Multifunctional On-board Power Processor with Multimode Capabilities for Electric Vehicle Applications*" by "*Virendra Prasad Maurya*" has been carried out under my supervision, and this work has not been submitted elsewhere for a degree.

It is further certified that the student has fulfilled all the requirements of Comprehensive, Candidacy and SOTA for the award of Ph.D. Degree.



Supervisor आचार्य / PROFESSOR
विद्युत् अभियंत्रिकी विभाग / Department of Electrical Engineering
भारतीय प्रौद्योगिकी संस्थान / Indian Institute of Technology
Prof. R. K. Singh (Banaras Hindu University)
Varanasi, U.P. (INDIA)

Professor

Department of Electrical Engineering

Indian Institute of Technology (BHU)

Varanasi-221005

DECLARATION BY THE CANDIDATE

I, **Virendra Prasad Maurya**, certify that the work embodied in this thesis is my own bonafide work and carried out by me under the supervision of **Prof. R. K. Singh** from **July 2019 to April 2025** at the **Department of Electrical Engineering**, Indian Institute of Technology (Banaras Hindu University), Varanasi. The matter embodied in this thesis has not been submitted for the award of any other degree/diploma. I declare that I have faithfully acknowledged and given credits to the research workers wherever their works have been cited in my work in this thesis. I further declare that I have not wilfully copied any other's work, paragraphs, text, data, results, *etc.*, reported in journals, books, magazines, reports dissertations, thesis, *etc.*, or available at websites and have not included them in this thesis and have not cited as my own work.

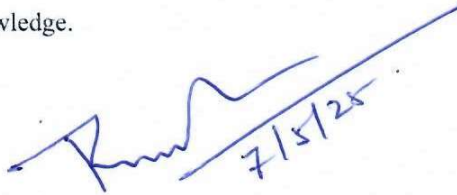
Date: 07/05/2025
Place: Varanasi



Signature of the Student
(Virendra Prasad Maurya)

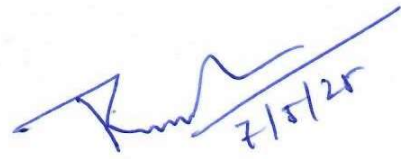
CERTIFICATE BY THE SUPERVISOR

It is certified that the above statement made by the student is correct to the best of my knowledge.



Head of Department

Department of Electrical Engineering
आचार्य व विभागाध्यक्ष / PROFESSOR & HEAD
विद्युतीय अभियंत्रिकी विभाग / Department of Electrical Engineering
भारतीय प्रौद्योगिकी संस्थान / Indian Institute of Technology
(बाराही हिन्दू विश्वविद्यालय) / (Banaras Hindu University)
Varanasi, U.P. (INDIA)



Supervisor

(Prof. R. K. Singh)
आचार्य / PROFESSOR
विद्युतीय अभियंत्रिकी विभाग / Department of Electrical Engineering
भारतीय प्रौद्योगिकी संस्थान / Indian Institute of Technology
(बाराही हिन्दू विश्वविद्यालय) / (Banaras Hindu University)
Varanasi, U.P. (INDIA)

COPYRIGHT TRANSFER CERTIFICATE


Title of the Thesis: Multifunctional On-board Power Processor with Multimode Capabilities
for Electric Vehicle Applications

Name of the Student: Virendra Prasad Maurya

Copyright Transfer

The undersigned hereby assigns to the Indian Institute of Technology (Banaras Hindu University) Varanasi all rights under copyright that may exist in and for the above thesis submitted for the award of the "*Doctor Of Philosophy*".

Date: 07/05/25
Place: Varanasi



Signature of the Student
(Virendra Prasad Maurya)

Note: However, the author may reproduce or authorize others to reproduce material extracted verbatim from the thesis or derivative of the thesis for the author's personal use, provided that the source and the Institute's copyright notice are indicated.

Acknowledgement

With profound gratitude and heartfelt joy, I write the acknowledgment section of my Ph.D. thesis—the final piece of this remarkable journey. At the very outset, I bow in reverence before Lord Shiva, whose divine presence led me to the sacred city of Varanasi and has remained a constant source of inspiration since the day of my IIT BHU entrance examination. This journey would not have been possible without the blessings of Baba Vishwanath, who bestowed upon me the wisdom, health, and strength to persevere and complete this thesis.

It is a great pride and pleasing privilege for me to express my gratefulness to “*Bharat Ratna Mahamana Pandit Madan Mohan Malaviya Ji*”, founder of this century old institute *Indian Institute of Technology, (BHU), Varanasi and Banaras Hindu University* at large for his creation of this serene varsity campus that provides me pleasant environment for carrying out my research work.

Undertaking this Ph.D. journey has been a truly life-changing experience, and it would not have been possible without the unwavering guidance and support of my supervisor, mentor, and Guru, *Prof. Rajeev Kumar Singh*. I express my deepest gratitude to him for his consistent encouragement, insightful suggestions, and steadfast dedication throughout my research. From foundational discussions on power electronics to intense technical brainstorming sessions, every interaction with him has been an invaluable learning experience. His wisdom, clarity, and at times, his firm correction of my misconceptions, have shaped not only my research but also my approach to learning and problem-solving. Prof. Singh is one of the most knowledgeable, experienced, and intellectually sharp individuals I have had the privilege to know. I aspire to emulate his enthusiasm, liveliness, and boundless energy in my own academic and professional journey.

I would like to express my heartfelt gratitude to, *Dr. Vivek Nandan Lal* and *Prof. Ranjit Mahanty* for their unwavering support and invaluable guidance throughout this journey. Their encouragement and steady presence have been pillars of strength, especially during challenging times, helping me remain positive and focused. I feel truly fortunate to have had mentors who not only offered insightful advice but were also actively engaged in reviewing and refining my research manuscripts. Their thoughtful suggestions and constructive feedback have left a lasting impact, and I will carry their wisdom with me as I move forward in my academic and professional path.

Most importantly, I would like to express my heartfelt gratitude to the esteemed professors whose collaborative efforts led to the founding of our research group, VLPERI (Virtuous Lab of Power Electronics Research & Innovation). I feel truly privileged to have been part of VLPERI since its inception. Their dedication to creating a supportive and stimulating research environment, with a focus on innovation, collaboration, and academic excellence, has played a significant role in shaping my academic journey. Despite their demanding schedules, they were always approachable and willing to address my technical queries, offering invaluable guidance throughout my research. I am deeply thankful for the opportunity to learn from their expertise and for the unwavering support they have provided. Thank you, Professors, for your vision, mentorship, and encouragement.

I would like to extend my sincere gratitude to **Dr. Jeevan Vachan Tirkey** (Department of Mechanical Engineering), **Dr. Tarun Verma** (Department of Mining Engineering), **Prof. Chhail Kumar Behara** (Department of Metallurgical Engineering), and **Dr. Naveen Yalla** (Department of Electrical Engineering) for enriching my journey beyond academics. Also, I would like to thank **Jeetu Bhaiya** for his guidance, which helped me to complete this journey. Their encouragement and guidance in teaching me how to play badminton not only improved my physical fitness but also strengthened my discipline, resilience, and mental well-being.

I deeply appreciate the efforts and support of all my fellow VLPERI group members, who have been an integral part of this journey. Beginning with my juniors, I would like to express my heartfelt gratitude to **Ankit Kumar Pratihasta** for his consistent support in experimental work, manuscript writing, and helping me refine my theoretical understanding. I also thank **Arya and Aman** for their valuable contributions to my research experiments and writing efforts. My sincere thanks to **Manish** for his assistance in component selection and to **Sagar** for being a constant source of support throughout every phase of my research.

I am especially grateful to my Ph.D. batchmates from VLPERI. **Dr. Priyatosh Jena** has been instrumental at every step, guiding me from the basics of signal transmission from the FOD to the switch, to managing the major circuit boards. I thank **Dr. Prakash Ji Barnawal** for being part of my early learning process, especially in understanding circuit operation, and later assisting me in manuscript and thesis writing. I sincerely thank **Dr. Warda Matin Khan** for her help in addressing paper revisions and manuscript preparation, and **Dr. Rajat Keshari** for his support with manuscript writing.

I would also like to extend my gratitude to my seniors for their foundational contributions to stabilizing the VLPERI lab, setting up the equipment, and teaching us how to communicate with hardware through microcontrollers. In particular, I thank **Dr. Soumy Ranjan Mehar** for teaching me the DSPF2833 microcontroller. My heartfelt thanks to **Dr. Pawan Kumar, Dr. Manas Kumar Mishra, Dr. Simanta Samal,** and **Dr. Soumya** for sharing their wisdom on lab management, inspiring teamwork, and maintaining discipline within the group. I am thankful to the lab staff, **Suresh Kumar Pal,** and **Chandra Bhaiya,** for all the help that can't be described in words. Thank you, everyone, for making this journey a sweet and memorable.

Last but not least, I would like to thank my family members for their patience with me and for giving me their support in this journey. Special thanks to **my MOM,** who is waiting for when my studies will be completed and when I will take responsibility for the family. I also thank my **younger brother,** who took responsibility for the family so that I could carry on my studies. I also thank my **elder brother** for their financial support in helping me complete this journey. Also, I would like to thank **my wife** for supporting me in every situation and compromising her desires in the competition of this journey.

I am also deeply grateful to everyone whose name I may have inadvertently omitted. Your unseen support has been invaluable in completing this journey.

List of Figures

Figure	Caption	Page Number
Fig.1. 1	Block diagram of the conventional EV system.	2
Fig.1. 2	Different possible integrated onboard chargers.	4
Fig.1. 3	On-board charger integrated with a multi-winding transformer for charging the main battery and a low-voltage battery charger.	5
Fig.1. 4	On-board charger integrated for voltage battery charger with a two-winding transformer.	5
Fig.1. 5	Couple magnetic-based integrated power unit that can provide two functionalities: (a) boost motor drive and (b) OBC.	6
Fig.1. 6	On-board charger is integrated and used as a V2V charger.	7
Fig.1. 7	A multifunctional power converter for G2V, V2G, and LVBC.	8
Fig.1. 8	Integrated circuit of on-board charger for G2V, V2G, and motoring operation.	8
Fig.1. 9	Integrated switch reluctance power train with OBC for G2V charging, LVB charging, and MM operation.	9
Fig.1. 10	Block diagram of the proposed power processor.	12
Fig.2. 1	Conventional EV system.	16
Fig.2. 2	Circuit diagram of the multifunction on-board power processor for electric vehicles.	18
Fig.2. 3	Circuit diagram of the M-OBNE during charging mode.	18
Fig.2. 4	Circuit diagram of the M-OBNEV in propulsion mode.	18
Fig.2. 5	Circuit connection for the V2V charging, a) circuit of the energy supplier vehicle, and (b) circuit of the energy acceptor vehicle.	19
Fig.2. 6	Operation of front-end PFC converter during positive cycle of source voltage, (a) S4-S6 is ON, (b) both switches are OFF, during negative cycle of the source voltage (c) S4-S6 are ON, (d) both switches are OFF.	19
Fig.2. 7	Three DC outputs are generated during the charging mode by M-OBNEV.	20
Fig.2. 8	(a) complete shoot-through operation, (b) inverter shoot-through operation, (c) power stage of the non-shoot-through interval, and (d) zero state of the non-shoot-through interval of the PPP.	22
Fig.2. 9	Control logic block diagram of battery charging.	26

Fig.2. 10 The control logic of charging mode: (a) control unit I maintains the unity power factor at the source terminal and charges the battery with CC-CV charging, (b) control unit II regulates the multioutputs for the auxiliary power supply.....	26
Fig.2. 11 Bode plot, (a) voltage control loop, and (b) current control loop.....	27
Fig.2. 12 (a) Pulse generation logic for modified SPWM, and (b) generated switching signals for modified SPWM.....	29
Fig.2. 13 Photograph of the proposed converter.	30
Fig.2. 14 In charging mode, (a) unity power factor with multioutputs, (b) CC-CV charging.	31
Fig.2. 15 In charging, (a) THD spectrum of source current, and (b) the available output voltages.	31
Fig.2. 16 In charging, (a) zero voltage switching with series resonance operation of the intermediate part of the PPP, and (b) voltage drop across switches SA and SB, with the inductor LA and LB current profile during multi-output operation.....	32
Fig.2. 17 (a) switching for the V2V energy transfer with inductor energy balancing, (b) load dynamics during V2V charging.	34
Fig.2. 18 Switching sequence S1, S4, S3, S6, and S5, S2, SB of the proposed power processor during propulsion mode.....	33
Fig.2. 19 (a) Inverter line voltage VAB and VBC with multioutput voltages V01 and V02, and (b) Inverter line voltages VAB, VBC, and VCA are 1200 phase-shifted from each other.....	33
Fig.3. 1 Block diagram of a BLDC motor drive with an adaptable multifunction power processor having multimode operation.	37
Fig.3. 2 Circuit diagram of a BLDC motor drive with an adaptable multifunction power processor having multimode operation.	37
Fig.3. 3 Circuit diagram of the proposed converter in charging mode.	37
Fig.3. 4 Circuit diagram of the proposed converter in motoring mode.	38
Fig.3. 5 HPLN switching scheme.	39
Fig.3. 6 Inverter operation in the high-frequency switching during of switch S ₁ , (a) inverter operation when switches S ₁ is being turned on, and S ₆ is already conducting, and (b) free-wheeling period of the inverter when switch S ₁ is turned OFF while S ₆ is already conducting.	39
Fig.3. 7 Switching sequence for FEC during charging mode.	41
Fig.3. 8 Switching sequence for the positive cycle of supply source, (a) when switches S ₄ , and S ₆ are ON, (b) when switches S ₄ , and S ₆ are OFF.....	41
Fig.3. 9 The reaction of the BLDC motor during the switching.....	41

Fig.3. 10 Switching sequence for the negative cycle of supply source, (a) when switches S_4 , and S_6 are ON, (b) when switches S_4 , and S_6 are OFF.....	42
Fig.3. 11 The reaction of the BLDC motor during the switching.....	42
Fig.3. 12 Circuit diagram of HB-LLC converter.	43
Fig.3. 13 Simulation result of the ZVS condition of HB-LLC switches S_5 and S_2	43
Fig.3. 14 Proposed converter operation for auxiliary power supply.....	44
Fig.3. 15 Circuit used for V2V charging, (a) circuit of energy supplier vehicle, and (b) circuit of energy acceptor vehicle.	44
Fig.3. 16 (a) Control technique of the BLDC motor speed control, and (b) control technique for auxiliary power supply.	46
Fig.3. 17 Conventional two-stage controller for EV charging.....	47
Fig.3. 18 Single-stage controller for EV charging.....	47
Fig.3. 19 Charging mode control of the proposed multimode on-board power converter.....	47
Fig.3. 20 Bode plot of voltage loop control.	48
Fig.3. 21 Bode plot of the current control loop.....	49
Fig.3. 22 Pictorial representation of the proposed converter.	52
Fig.3. 23 The output waveform of hall-effect position sensors	53
Fig.3. 24 HPLS for BLDC motor drive, (a) upper leg, and (b) for lower leg of the inverter. .	53
Fig.3. 25 Switching sequence of switches S_1 , S_3 at (a) speed 2100 rpm, (b) 1900 rpm.	54
Fig.3. 26 (a) Inverter line voltage in motoring operation and (b) auxiliary output voltages and line voltage V_{AB}	54
Fig.3. 27 Experimental validation of the proposed HPLS scheme demonstrating elimination of commutation current ripple from current $I'A$	55
Fig.3. 28 (a) The switching sequence of the boost PFC in charging mode and its zoomed view are shown in (b).	55
Fig.3. 29 (a) Unity power factor with auxiliary power supply V_{01} and V_{02} and (b) THD spectrum of the source current.....	56
Fig.3. 30 (a) HB-LLC operation, and (b) available outputs during the charging operation. ...	57
Fig.3. 31 S_A , S_B switching with inductor L_A and L_B current profile I_{LA} and I_{LB} , respectively, (b) stable voltage regulation in motoring mode during load dynamic.....	57
Fig.3. 32 Voltage and current profile of an energy supplier vehicle's battery, and current and voltage profile of an energy acceptor vehicle at a resistive load in place of the battery.....	58

Fig.4. 1 Conventional EV operations by different power converters with an additional 12 V battery.....	60
Fig.4. 2 Block diagram of the proposed converter.....	61
Fig.4. 3 Multioperation of the proposed converter, (a)1- Φ charging, (b) motoring, and (c) V2V charging.....	61
Fig.4. 4 Circuit diagram of the proposed power converter.	62
Fig.4. 5 proposed converter during single-phase charging.	62
Fig.4. 6 Proposed converter during motoring operation.	62
Fig.4. 7 Connection of the proposed converters for V2V charge transfer.	63
Fig.4. 8 control logic of the proposed system, (a) for the power factor correction, (b) for the regulated auxiliary power supply voltage, (c) BLDC motor drive operation, and (d) acceptor vehicle control logic.....	69
Fig.4. 9 Bode plot of the uncompensated and compensated high-power auxiliary voltage.	70
Fig.4. 10 Bode plot of the uncompensated and compensated of low-power auxiliary voltage.	70
Fig.4. 11 Map of the proposed converter loss distribution during charging mode.	75
Fig.4. 12 Map of the proposed converter loss distribution in motoring mode.....	76
Fig.4. 13 map of the proposed converter loss distribution during V2V charging.....	76
Fig.4. 14 Efficiency curve of all the modes of operations.	77
Fig.4. 15 Photograph of an experimental prototype of the proposed converter.....	77
Fig.4. 16 During AC charging, (a) available output voltages for battery and cabin’s power demand and (b) unity power factor with the auxiliaries’ voltages.....	78
Fig.4. 17 (a) THD spectrum of the source current and (b) intermediate resonant converter operation during series resonance.....	79
Fig.4. 18 CC-CV charging operation.....	79
Fig.4. 19 In single-phase charging, (a) the power factor (PF) at the source terminal is maintained during load dynamics, and (b) the available voltage is sustained after load dynamics are applied at high-power auxiliary.	80
Fig.4. 20 (a) represents motor line current i_a , i_b , i_c , with battery voltage (b) represents battery input current with voltage across the switch (V_{DS})......	81
Fig.4. 21 (a) Inverter switch current of one-leg when driven with High-PWM Low-ON switching scheme, (b) Multioutput with line voltage (VAB) during motoring operation.	81
Fig.4. 22 Load dynamic during motoring mode, (a) Load dynamic at high-power auxiliaries, and (b) Load dynamic at the low-power auxiliaries.	82

Fig.4. 23 Dynamic result of the proposed converter during motoring mode(a) load dynamics in high-power auxiliaries, and (b) change in the speed of the motor.	82
Fig.4. 24 (a) The inductors L_A and L_B flux balance with respect to drain to source voltage of switch S_A , and S_B , during multioutput and (b) S_A , S_C switching voltages V_{A-DS} , V_{C-DS} , and according to them, the inductor L_A 's currents $I_{LA-Supplier}$, $I_{LA-Acceptor}$, charging.	83
Fig.4. 25 V2V operation of the proposed converter, (a) Available voltages during V2V charging, and (b) simultaneously applied the load dynamics in the low-power and high-power auxiliaries.	84
Fig.4. 26 Current sharing between 72 V and 12 V during different load conditions, (a) current sharing of high-power auxiliaries unaffected by variation in a load of low-power auxiliaries, (b)current sharing of low-power auxiliaries unaffected by variation in a load of high-power auxiliaries.	84
Fig.4. 27 Thermal image of the proposed converter, (a) starting of the converter, and (b) after half an hour of the converter's operation.	85
Fig.5. 1 Purpose of different converters and their operation in a conventional system.	87
Fig.5. 2 Integrated on-board chargers with different functionalities.	88
Fig.5. 3 Circuit diagram of the proposed power converter.	88
Fig.5. 4 Circuit diagram of the proposed converter in single-phase charging and vehicle-to-grid power supply.	89
Fig.5. 5 Circuit diagram of the proposed converter in motoring mode.	89
Fig.5. 6 The connection of the circuit diagram from both vehicles during V2V charging, (a) circuit of energy supplier, and (b) circuit of energy acceptor.	90
Fig.5. 7 Flowchart for implementation of on-board charger in respective mode, and (b) user selection of their respective mode.	90
Fig.5. 8 (a) Simulation result of the current of BLDC field winding during single-phase charging, and (b) phase diagram of the current in phases (a) and (b).	91
Fig.5. 9 control logic of the proposed power processor, (a) control logic for unity power factor with CC-CV charging, (b) control logic for auxiliary power supply, (c) control logic for motor drive, (d) control logic for V2G power supply, and (e) control logic for energy acceptor vehicle.	93
Fig.5. 10 Bar chart of the cost comparative analysis with similar prior work.	97
Fig.5. 11 Experimental setup of the proposed converter.	98
Fig.5. 12 G2V operation of the proposed power processor, (a) PFC with the auxiliary power supply, and (b) THD spectrum of the source current.	99

Fig.5. 13 Load dynamics in G2V operation, (a) during PFC operation, and (b) stable voltage regulation during load dynamics in auxiliaries.	100
Fig.5. 14 V2G power supply by the proposed converter.	100
Fig.5. 15(a) converter line current i_a , i_b , and i_c with battery voltage during motoring operation, and (b) converter switch current of one-leg with drain to source voltage on switch S1, while driven with High-PWM Low-ON switching scheme.	101
Fig.5. 16 In motoring mode operation, (a) line voltages and (b) auxiliary voltages with the line voltage of the proposed converter.	101
Fig.5. 17 Load dynamics during motoring operation, (a) load dynamic is applied in the high-power auxiliaries, and (b) load dynamic is applied in the low-power auxiliaries.	102
Fig.5. 18 (a) V_{A-DS} and V_{B-DS} are the drain-to-source voltages of the switch S_A and S_B with the inductor L_A and L_B current profile of the energy supplier vehicle, and (b) energy supplier and acceptor vehicles' battery voltages with inductor current profile and drain-to-source voltage (V_{C-DS}) of the switch S_C of the energy acceptor vehicle.	103
Fig.5. 19 V2V charging operation, (a) available voltages, and (b) constant current charging of the acceptor vehicle remains sustained while a resistive load transient is applied to the acceptor vehicle battery terminal.	103
Fig.6. 1 Circuit diagram of the proposed power processor.	105
Fig.6. 2 Flowchart for the operation of the proposed power processor.	106
Fig.6. 3 Circuit diagram of the proposed power processor in single-phase charging.	107
Fig.6. 4 Circuit diagram of the proposed power processor in V2G operation.	107
Fig.6. 5 Circuit connection of the proposed power processor during V2V charging.	108
Fig.6. 6 Circuit diagram of the proposed converter in motoring mode.	109
Fig.6. 7 Control logic of the proposed power processor.	111
Fig.6. 8 Phase lock-loop for synchronizing angle.	111
Fig.6. 9 Efficiency curve of G2V operation.	113
Fig.6. 10 Efficiency curve of V2G operation.	114
Fig.6. 11 Efficiency of the curve during V2V charging.	115
Fig.6. 12 Efficiency curve during motoring mode operation.	115
Fig.6. 13 Photograph of the proposed power processor experimental setup.	116
Fig.6. 14 In charging, (a) PFC with auxiliary power supplies, and (b) THD spectrum of the source current.	117
Fig.6. 15 In charging, (a) voltage across the switch S1, S3, S4 and S6, and (b) PF during load dynamic.	117

Fig.6. 16 During V2G power supply, the grid voltage (V_{grid}), grid injected current ($I_{grid-inj}$), battery voltage (V_{bat}), and battery current (I_{bat}). 118

Fig.6. 17 In V2V charging, (a) load dynamics in the energy supplier vehicle, and (b) load dynamics in the energy acceptor vehicle. 118

Fig.6. 18 In motoring mode operation, (a) line voltage V_{AB} , DC-link Voltage, battery voltage, and current, and (b) line voltage with i_a , i_b , and i_c three-phase line current..... 119

List of Tables

Table	Caption	Page Number
Table 1. 1	Benefits of the adoption of the lithium-ion-based EV	1
Table 2. 1	Comparative analysis with similar prior work.....	17
Table 2. 2	Rating of the selected components.....	25
Table 2. 3	Design specification of the proposed converter	30
Table 3. 1	Six-step High-PWM Low-ON switching for BLDC motor drive.....	40
Table 3. 2	Comparative analysis with similar prior work.....	50
Table 3. 3	Cost comparative analysis.....	51
Table 3. 4	Specification of the proposed converter.....	52
Table 4. 1	Rating of the selected elements.....	66
Table 4. 2	Specification of the power level in their respective modes of operation	68
Table 4. 3	Comparative analysis with similar prior work.....	72
Table 4. 4	Cost comparative analysis.....	73
Table 4. 5	Formulation of the basic power electronics converter losses	74
Table 4. 6	Loss during single-phase charging operation.....	74
Table 4. 7	Loss during motoring mode (MM) operation	75
Table 4. 8	Proposed converter loss during V2V charging	76
Table 5. 1	Specification of the power level in their respective mode of operation.....	92
Table 5. 2	Comparison with functions and switch counts in similar prior works.....	96
Table 5. 3	Comparison of CUF in their respective modes	98
Table 5. 4	Available rated voltage in their respective mode of operation.....	98
Table 5. 5	Specification of components used in the proposed converter.....	98
Table 6. 1	Operation of the proposed power processor at its rated value	109
Table 6. 2	Comparison with similar prior work.....	112
Table 6. 3	Specification of the components used in the proposed power processor.....	116

List of Acronyms

AGM	Absorbed Glass Mat
AI	Artificial intelligence
BLDC	Brushless DC motor
CC	Constant current
CC	Common connector mode
CM	Common contact
CM	Charging connector mode
CUF	Component utilization factor
CV	constant voltage
DAB	Dual active bridge
DCR	DC resistance
EMC	Electromagnetic Compatibility
EMI	Electromagnetic interference
ESR	Equivalent Series Resistance
EV	Electric Vehicle
FEC	Front-end converter
G2V	Grid-to-vehicle
GM	Gain Margin
HB-LLC	Half-bridge LLC
HPLN	High-PWM low-ON
HPLS	High-PWM Low-ON switching
HVB	High-voltage battery
ICE	internal combustion engine
IM	Induction motor
IM	Induction motor
LV	Low-voltage
LVB	Low-voltage battery
LVBC	Low- voltage battery charger
MM	Motoring mode
MM	Motoring connector mode
M-SPWM	Modified sinusoidal pulse width modulation
NC	Normally closed contact
NC	Normally closed contact
NO	normally open contact
OBC	On-board charger
PCB	Perforated circuit board
PF	Power factor
PFC	Power factor correction
PI	Proportional integral
PLL	Phase lock loop
PM	permanent magnet
PM	Phase margin

PMSM	Permanent Magnet Synchronous Motor
PPP	Proposed power processor
PR	Proportional-resonant
PV	Photovoltaic
PWM	Pulse width modulation
Q-ZSI	Quasi-Z source inverter
RMS	Root mean square
SOC	state of charge
SPDT	Single-pole double-throw
SPST	Single-pole single-throw
SRM	Switch reluctance motor
THD	Total harmonic distortion
THD-F	Total Harmonic Distortion (THD) as a percentage of the Fundamental RMS value of the waveform.
THD-R	Total Harmonic Distortion (THD) as a percentage of the Root Mean Square (RMS) value of the waveform
UPF	unity power factor
V2G	Vehicle-to-Grid
V2H	Vehicle-to-Home
V2V	Vehicle-to-vehicle
VSI	Voltage source inverter
ZVS	Zero voltage switching